CrossMark

TECHNICAL PAPER

Separated pivot-shaft actuator for small skew angle in hard disk drives

Shinji Koganezawa[1] · Hiroshi Tani[1] · Norio Tagawa[1]

Abstract A large skew angle in a hard disk drive (HDD) adversely affects the flying stability of the head sliders and the off-track capability of the read/write head. A novel actuator in the form of a separated pivot-shaft actuator (SPA) with a small skew angle is proposed in this paper. The SPA was particularly designed for a four-disk 3.5-in. HDD and has a skew angle of $\pm 1.6°$, which is approximately one-tenth of that of a conventional voice coil motor. The SPA was numerically analyzed by a finite element method, and its mechanical characteristics were compared with those of a long-arm actuator (LAA) (which is a strong candidate for a small-skew-angle actuator) with respect to the seek performance and frequency response. It was found that the SPA had a higher resonant frequency, which enabled the achievement of a wider servo-bandwidth compared to the LAA, and that the average seek time of the SPA was significantly shorter than that of the LAA.

1 Introduction

Rotary-type voice coil motors (VCMs) are currently exclusively used in hard disk drives (HDDs). A rotary VCM has a skew angle, which is the angle between an axis perpendicular to the head width and an axis in the longitudinal direction of a track (see Fig. 1; Sect. 2 for details). The skew angle varies with the track from the inner diameter (ID) to the outer diameter (OD), and approximately ranges between $-15°$ and $+15°$ in a typical 3.5-in. HDD. It is well known that a large skew angle adversely affects the flying stability of the head sliders and the off-track capability of the read/write head (He et al. 2002). It has been recently considered that a large skew angle deteriorates the quality of the read-back signal of two-dimensional magnetic recording (TDMR) (He et al. 2013), which is a promising technology for achieving higher areal density. A reduction of the skew angle is thus highly desirable, and many studies have been conducted on rotary-VCM-based actuators with a small skew angle.

Rotary-VCM-based actuators can be categorized into two groups. The first group includes mechanisms in which the skew angle varies by only a small amount. The four-bar-linkage mechanism actuator (Chainer et al. 1991; Limmer et al. 2006; He et al. 2013) and long-arm actuator (LAA) (Yoshikawa et al. 1996; He et al. 2013) are examples of such actuators. The mechanisms of this type of actuators can reduce the variation of the skew angle to within 0.4°–4° but cannot entirely eliminate it. The second group includes actuators with skew angle compensation by means of slider-driven MEMSs. Electrostatic (Sarajlic et al. 2010) and electrothermal actuators (Messner et al. 2009) are examples of such actuators, and have been studied for compensation to achieve zero skew angle. Such MEMS actuators, however, have poor shock resistance because they are usually constructed with thin beams for supporting the slider. Based on several previous studies, LAAs are considered to be leading candidates for application to commercial HDDs because they are minimally different from conventional VCMs. Figure 2 is a schematic of an LAA. For example, the carriage arm is extended by only approximately 20 % compared to that of a VCM, and the head suspensions are fixed with a slant angle φ to minimize the absolute skew angle. It has, however, been reported that the long arm of an LAA reduces the arm-sway mode frequency

✉ Shinji Koganezawa
  skoga@kansai-u.ac.jp

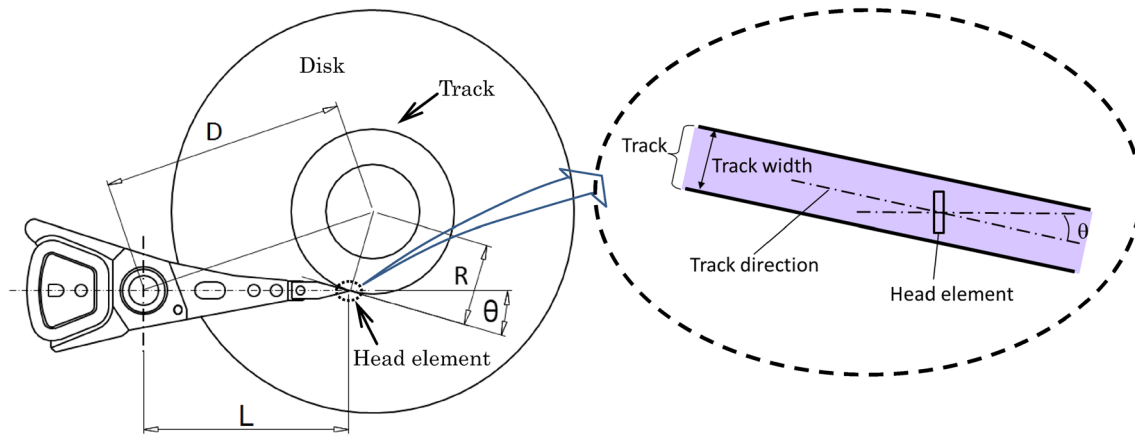[1] Department of Mechanical Engineering, Kansai University, 3-3-35 Yamate-cho, Suita-Shi, Osaka, Japan
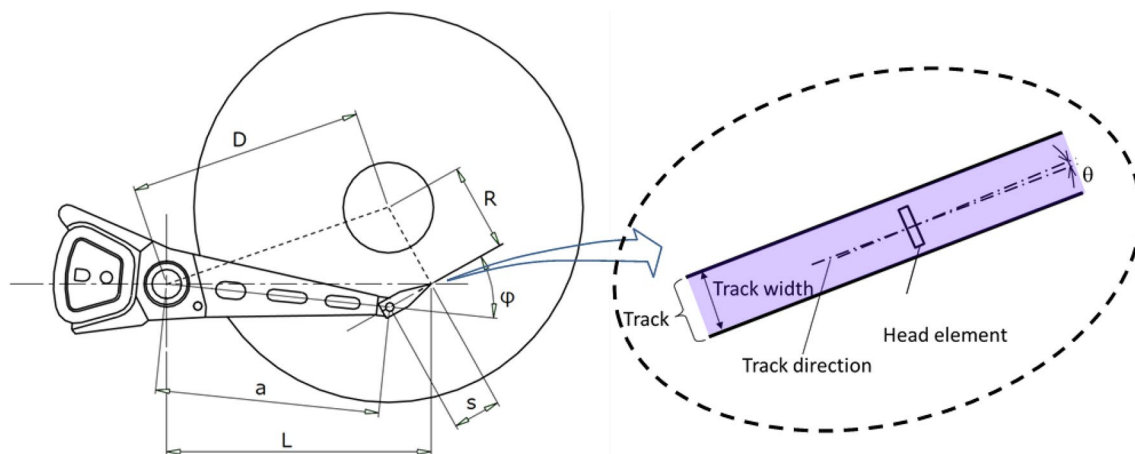
Fig. 1 Illustration of the skew angle

Fig. 2 Schematic of an LAA and the slant angle

by 20–30 % (He et al. 2002). In addition, the moment of inertia of an LAA is substantially larger than that of a VCM, and this significantly reduces the seek performance. Mechanical designers of HDD manufacturers are thus reluctant to use LAAs in commercial HDDs.

In the present study, a novel rotary VCM in the form of a separated pivot-shaft actuator (SPA) was developed. The SPA has a small skew angle comparable to that of an LAA, but better frequency response and seek performance. The mechanical characteristics of the SPA were investigated by a finite element method (FEM) and compared with those of an LAA and a VCM.

2 Structure of SPA

Before describing the structure of the proposed SPA, the author would like to discuss the skew angle with reference to Fig. 1. As mentioned above, the skew angle θ is the angle

between an axis perpendicular to the head width and an axis in the longitudinal direction of a track. It is geometrically given by

$$\theta = \sin^{-1}\left(\frac{L^2 + R^2 - D^2}{2LR}\right) \qquad (1)$$

where L is the distance between the actuator pivot and the head element, D is the distance between the centers of the spindle and the pivot, and R is the radius of the data track on which the head is positioned. As indicated by Eq. (1), θ is a function of R. In the case of a typical 3.5-in. HDD with the L and D dimensions given in Table 1, the skew angle θ varies approximately between $-15°$ and $+15°$. The skew angle variation, which is the difference between the maximum and minimum values, is thus approximately 30°. Because the ID and OD of the data track are usually determined by the HDD specifications, the mechanical parameters that determine θ are L and D.

Table 1 Specifications of HDD

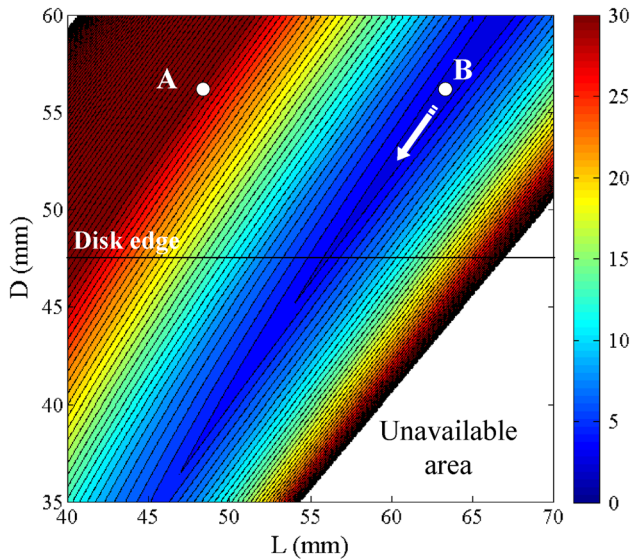| Parameter	Value
HDD form factor	3.5 in.
Number of disks	4
Disk diameter	95 mm
Data zone diameter	ID: 38.8 mm
	OD: 90.2 mm

Fig. 3 Contour plot of the variation of the skew-angle

Figure 3 shows a contour plot of θ variation with respect to the parameters in Table 1. The horizontal and vertical axes, respectively represent L, and D. The point A specifies the dimensions of the VCM, and the skew angle variation is approximately 30°, as noted earlier. In the general procedure for designing an LAA, L is increased by increasing the carriage arm while maintaining the length D. This is done to enable the use of the same ball bearings used in a VCM. Point B specifies the optimized design of an LAA from the perspective of minimum skew variation. The variation of θ has a minimum value of 2.8° for L = 63.6 mm. Once the design value of L for a small θ variation is obtained, the absolute skew angle can be minimized by the appropriate slant angle φ, which is the angle between the longitudinal axis of the carriage arm and the axis of the head suspension as shown in Fig. 2. It should be noted that the distance s between the center of the swage hole and the head is usually fixed by the specifications of the head suspension. The arm length a and φ are given by the following equations in terms of the determined values of L, D, and θ.

$$a = \sqrt{L^2 + s^2 - 2Ls\cos\theta_s} \tag{2}$$

$$\varphi = \cos^{-1}\left(\frac{L^2 - a^2 - s^2}{2as}\right) \tag{3}$$

$$\theta_s = \frac{\theta_{max} - \theta_{min}}{2} \tag{4}$$

where θ_s is the offset angle used to minimize the absolute skew angle, and θ_{max} and θ_{min} are, respectively the maximum and minimum values of θ within the range of R (the distance between the ID and OD).

The mass and the moment of inertia of an LAA significantly increase with the length of the longer arm and any additional mass used for mass balance (i.e., any additional mass used to adjust the center of mass of the rotary VCM about the pivot axis). A shorter arm is therefore desirable to improve the mass properties. However, it can be seen from Fig. 3 that the variation of θ increases with the shortening of the arm.

A valley line can be observed in the contour plot in Fig. 3. The valley line indicates a set of optimized design values of L and D. Figure 4 shows the trend of the variation of θ when L and D move along the valley line, and this can also be used to determine the minimum variation of θ with respect to L. When L decreases below 63.6 mm, which is the value required for the LAA, the variation of θ increases by no more than 2°, which is insignificant compared to the variation of θ in current conventional VCMs. Therefore, when both L and D are shortened along the valley line from point B, the arm length can be decreased while maintaining a small variation of θ. However, when shortening D in a conventional VCM, there is interference between the magnetic disks and the pivot bearings or the carriage.

Figure 5 is a schematic of the concept of the proposed SPA. There are two sets of pivot bearings, and they are fixed to the top and bottom arms, respectively. Each pivot
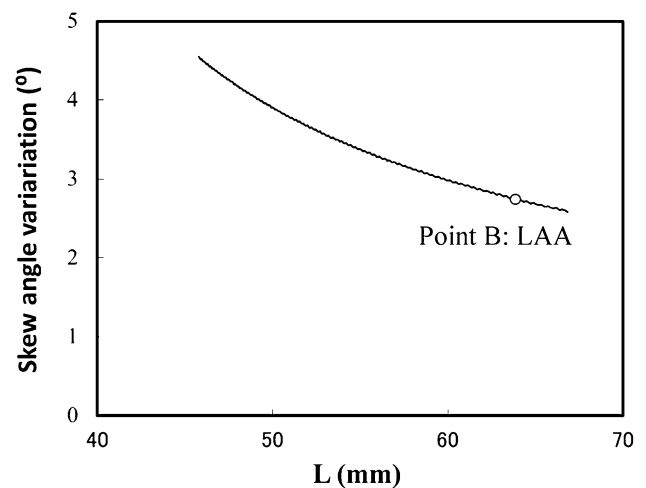

Fig. 4 Minimum variation of the skew-angle with respect to L
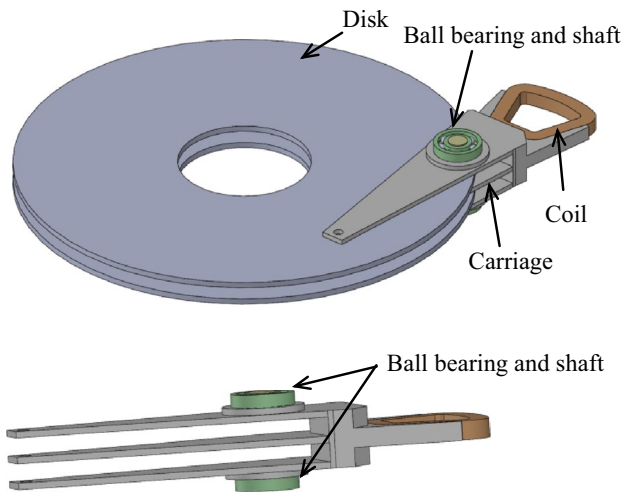
Fig. 5 Concept of the separated pivot-shaft actuator

shaft is fixed on the inner sleeve of each ball bearing set, and also fixed to the base or cover of the HDD. Part of the VCM carriage sandwiched between the pivot bearings is cut out to avoid interference with the magnetic disks. In the figure, the dimensions of the ball bearings and the cutout of the carriage are a little exaggerated to aid understanding. Based on this concept, D can be designed to be shorter than that of a conventional VCM or LAA using the same size of ball bearings and without the interference associated with the shortening in a conventional VCM. In addition, the mass and moment of inertia can be reduced compared to those of an LAA because the arm is shorter and it is easy to adjust the center of mass on the pivot axis without using additional mass.

3 Actuator design

The values of L, D, and s (see Fig. 3) of the VCM were first determined as given in Table 2. The designed VCM is shown in Fig. 6a. Simplifications of the head suspensions are shown in Fig. 6 to facilitate illustration of the slant angle φ and the locations of the heads, which are indicated by their tips. The size of the ball bearings was assumed to be $\phi11$ mm $\times$ $\phi7$ mm $\times$ 2.5 mm thick.

The LAA was then designed by increasing the carriage arms compared to those of the VCM and applying an adequate slant angle to minimize the absolute skew angle. The essential parameters a, φ, and θ variation were calculated using Eqs. (1)–(4) as shown in Table 2. The center of mass of the LAA was adjusted to position it close to the pivot axis by increasing the size and thickness of the coil. The LAA is shown in Fig. 6b. As indicated in Table 2, the long

Table 2 Design parameters of the actuators

Specifications	VCM	LAA	SPA
Spindle-to-pivot distance D (mm)	56.3	56.3	48.5
Pivot-to-head distance L (mm)	48.2	63.6	56.8
Swage-to-head distance s (mm)	11.4	11.4	11.4
Pivot-to-swage distance a (mm)	36.8	53.92	47.58
Slant angle φ (°)	0	35.0	39.9
Mass m (g)	14.59	21.22	17.19
Moment of inertia J (gmm^2)	4278	10,505	7241
Travelling angle α (°)	30.9	26.4	30.7
Effective radius of gyration of the coil R_{coil} (mm)	17.7	19.5	21.5
Skew angle variation (°)	30.5	2.8	3.2
Average seek time ratio	1	1.35	1.18

arm and larger coil used for the mass balance of the LAA significantly increased the mass and moment of inertia. The resultant moment of inertia was 2.5 times that of the VCM. The average seek time was calculated using

$$t_{Ave} \propto \sqrt{\frac{J\alpha}{R_{coil}L}} \qquad (5)$$

where R_{coil} is the effective radius of gyration of the coil, α is the travelling angle of the read/write heads between the ID and OD, and J is the moment of inertia. Assuming that the torque constants of the electromagnetic forces of the two actuators are the same, the average seek time of the LAA would be 1.35 times that of the VCM (see Table 2).

The SPA was finally designed by shortening the L and D of the LAA so that they were on the valley line in Fig. 3 as noted in Sect. 2. The optimal values of L and D for which the center of mass of the SPA would be near the pivot axis were determined by trial and error. It should be noted that a wider coil than that of the VCM is required if the actuator pivot moves away from the coil owing to the larger radius of gyration of the coil that would result. This introduces a little complication into the design of the SPA. The distance D between the center of the spindle and the pivot axis was designed to be 48.5 mm, which resulted in the pivot axis being 1 mm from the edge of the magnetic disk. A θ variation of 3.2° was achieved, which is approximately one-tenth of that of the VCM. The part of the carriage between the ball bearings was cut out to prevent the carriage from interfering with the magnetic disks, as shown in Fig. 6c. The size of the ball bearings of the SPA was the same as those of the VCM and LAA. The SPA carriage was, however, 1.5 mm thicker than the other carriages because the axial distance between two ball bearings had to be wider than the thickness of the stacked disks on a spindle motor
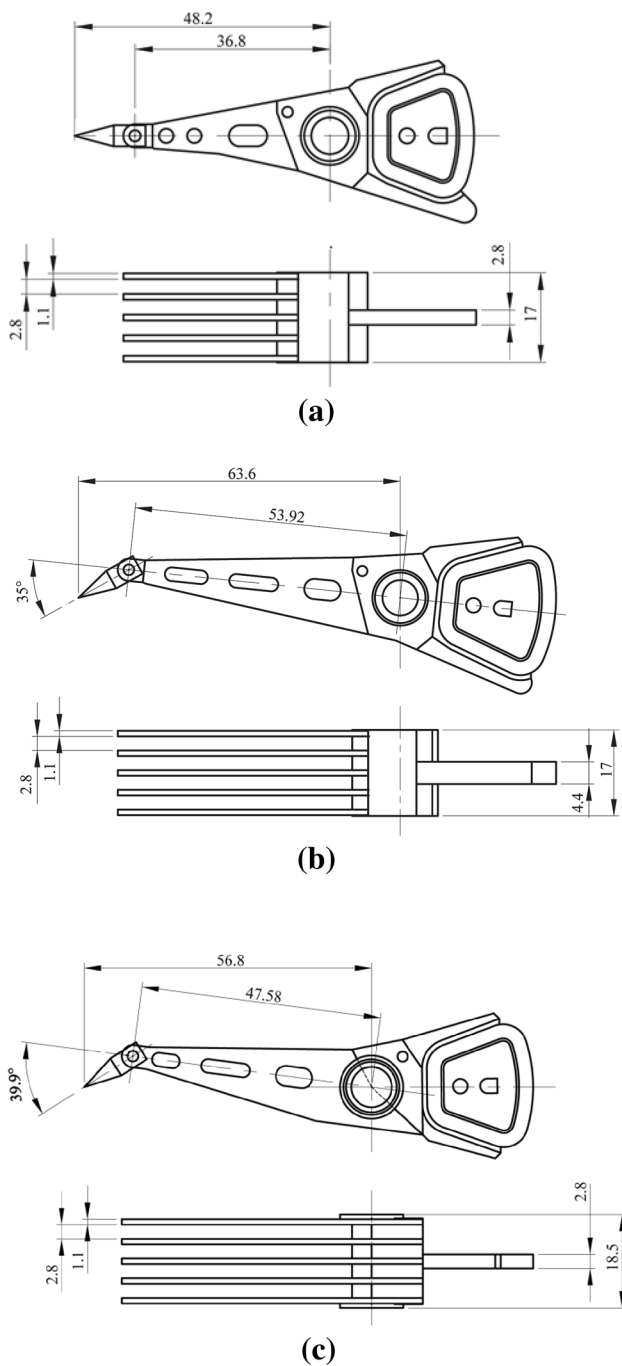
(a)

(b)

(c)

Fig. 6 Rotary actuators designed in the present study. **a** VCM, **b** LAA, **c** SPA

to prevent interference between the disks and ball bearings. The increase in the carriage thickness is the drawback of the SPA of a multi-disk HDD. In addition, because the moment of inertia is decreased by 31 % compared to that of the LAA, the average seek time is shortened by 12.6 %, although it is still longer than that of the conventional VCM.

4 FEM analysis

ANSYS 15.0 was used to perform an FEM analysis to investigate the frequency response functions (FRFs) of each actuator. In the finite element models, each head suspension was modeled as a mass point of mass 50 mg and placed at the center of the swage holes. This was based on a previous report that a head suspension with a slant angle had little effect on the resonance modes (He et al. 2002). Two ball bearings of the same type were used for each of the three actuators, namely, the SPA, VCM and LAA. The radial and axial stiffness of each bearing were assumed to be 1.8×10^7 and 6.0×10^6 N/m, respectively. The stiffness of each bearing was modeled by linear springs as shown in Fig. 7, with k_x, k_y, and k_z set to 9.0×10^6, 9.0×10^6, and 1.5×10^6 N/m, respectively. The bearing span of the SPA was 17 mm and those of the VCM and LAA were 14.5 mm. The difference was because of the thick structure of the SPA as mentioned above. The HDD housing comprising the HDD base and the cover were not modeled, and the pivot shafts were fixed to the ground as the boundary condition for the FEM analysis.

Figure 8 compares the FRFs of the three actuators when excited by an electromagnetic force at each coil. Because the structures of the actuators have a plane symmetry, the FRFs of the top arm and bottom arm are almost the same for the three actuators. In addition, there were no significant differences among the FRFs of the other three middle arms. Hence, only the FRFs of the top and middle arms are shown in Fig. 8.

In the FRFs of the VCM, the dominant resonance for servo-bandwidth limitation is the butterfly mode at 6.2 kHz, and this is mainly determined by the mass and lateral stiffness of the ball bearings. Regarding the FRFs of the LAA, the dominant resonance is also the butterfly mode at 4.6 kHz, although the highest peak in the FRF of the top arm is the arm-sway mode at 5.0 kHz. The increased mass of the LAA caused the frequency of its butterfly mode to drop by 1.6 kHz.

In the SPA, the free lengths of the top and bottom arms are shorter than those of the other arms because the top and bottom arms are supported by ball bearings on the front side. The FRFs of the top and middle arms are therefore significantly different. The dominant resonance in that of the top arm is the arm-sway mode at 5.8 kHz, although there is a small peak that corresponds to the butterfly mode at 5.1 kHz. The reason for this is that the amplitude of the butterfly mode of the top and bottom arms is very small whereas that of the arm-sway mode is large, as shown in Fig. 9. In the case of the FRF of the middle arm, the dominant resonance is the butterfly mode at 5.1 kHz. Compared to the LAA, the dominant resonance frequencies of the top and middle arms of the SPA are increased by 1.2 and 0.5 kHz, respectively.

Fig. 7 Simulation model of the ball bearing. **a** Schematic of ball-bearing, **b** ball-bearing model with linear springs
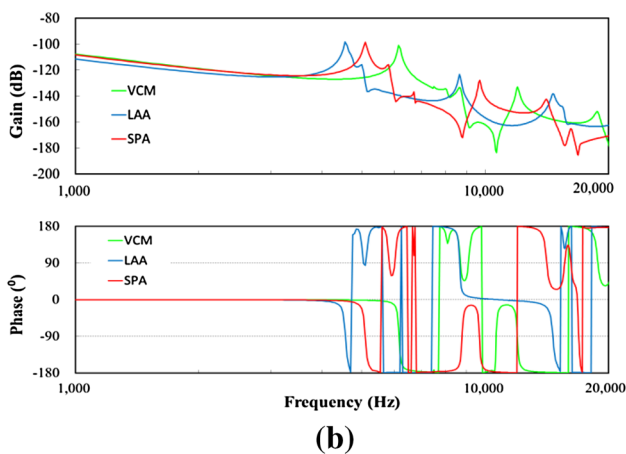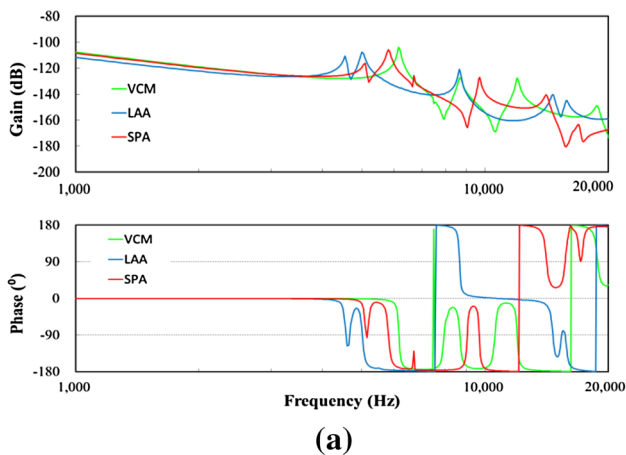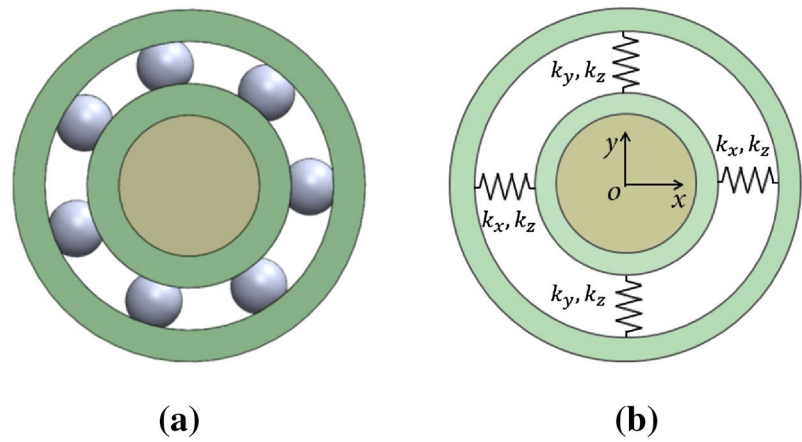

(a)   (b)

(a)

(b)

Fig. 8 FRFs of the actuators. **a** Top arm, **b** middle arm

Fig. 9 Butterfly and arm sway modes of the SPA

It is considered that the stiffness of the HDD housing of the SPA affected the mechanical characteristics such as the FRFs because the pivot shaft of the SPA was structurally separated. We also calculated the tilt angle of the carriage when a force of 10 N was applied to the top surface of the upper pivot shaft while the lower pivot shaft was fixed to the ground. This was used to consider a case in which the top cover is deformed. The tilt angle of SPA was determined to be 9.6×10^{-4} rad, which is 26 times those of the VCM and LAA (3.7×10^{-5} rad). This is because the 10 N force directly acts on the ball bearings of the SPA, whereas the bending stiffness of the pivot shaft reduces the force that is transmitted to the ball bearings of the VCM or LAA. The FRFs are, however, not significantly affected by the tilt produced by a static force of 10 N because the tilt angle of the SPA is very small, as is also the case in both the VCM and LAA. The tilt angle increases with decreasing bearing span.

Another issue of concern regarding the SPA is the reduction in the pre-load of the ball-bearing with the deformation of the HDD cover when the upper pivot shaft is fixed to the cover. The use of a rigid bridge between the upper pivot shaft and the HDD base, or the yoke of the magnetic circuit, may eliminate the need to fix the upper pivot shaft to

The other major resonance-mode frequencies are also given in Table 3. Regarding the top arm of the SPA, owing to its being shorter, the resonance frequencies of all the major modes are improved compared to those of the LAA, although they are lower than those of the VCM, being the trade-off for the small skew angle.
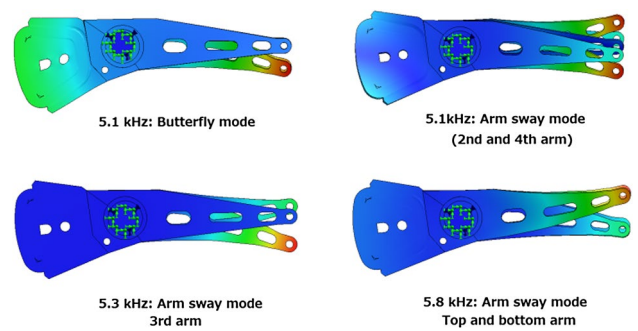
Table 3 Resonance mode frequency (Hz)

Resonance mode	VCM	LAA	SPA
Arm bending	980–1140	470–520	T: 640
			M: 510
Butterfly	6.2 k	4.6 k	5.1 k
Arm sway	8.0–8.9 k	4.4–5.2 k	5.1–5.8 k
Arm torsion	10.2–11.8 k	5.5–5.6 k	T: 5.9 k
			M: 4.8–5.0 k

T top arm, *M* middle arm

the HDD cover. However, the use of the rigid bridge would further increase the thickness of the SPA structure because of the space required to accommodate the bridge between the upper pivot shaft and the HDD cover. This thickness issue can be regarded as an overall structural drawback of the SPA.

5 Conclusion

A novel rotary VCM in the form of a separated pivot-shaft actuator (SPA) with a small skew angle was proposed. The SPA was particularly designed for a 3.5-in. HDD and was numerically analyzed by a finite element method (FEM). Its mechanical characteristics were compared with those of a conventional VCM and long-arm actuator (LAA). The SPA has a skew angle of ±1.6°, which is approximately one-tenth of that of the conventional VCM and almost the same as that of the LAA. Because the dominant resonance frequency of the SPA is higher than that of the LAA, the SPA can have a wider servo-bandwidth compared to the LAA in addition to its small skew angle. The drawback of the SPA appears when it is used for a multi-disk HDD, and

this consists in the possibility of the carriage height being thicker than those of the VCM and LAA. This is because the axial distance between the two ball bearings must be wider than the thickness of the stacked disks on the spindle motor to prevent interference between the disks and the ball bearings. Considering this drawback, and in the light of the FEM results that revealed that the FRFs of the top and bottom arms of the SPA are superior to those of the middle arms, the SPA is particularly suitable for few-disk HDDs, especially one-disk HDDs.

References

Chainer TJ, Sohn VJ, Sri-Jayantha M, Brown DH, Apuzzo NC (1991) A flexural in-line actuator for magnetic recording disk drives. IEEE Trans On Magn 27(6):5295–5297

He Z, Ong EH, Guo G (2002) Optimization of a magnetic disk drive actuator with small skew actuatio. AIP J Appl Phys 91(10):8709–8711

He Z, Mou J, Chan KS, Lam SH, See BL, Lin W (2013) A near zero skew actuation mechanism for hard disk drives. ASME Proceedings of ISPS 2013, 24–25, ISPS 2013-2941

Limmer JD, Boutaghou ZE, Bonin WA (2006) Hard drive actuator arm with reduced skew variation. USP US 7,072,147 B2

Messner WC, Bain JA, Koenders M, Groenesteijn J, Marsman GH, Gilgunn PJ, Fedder GK (2009) A CMOS-MEMS rotary microactuator suitable for hard disk drive applications. IEEE Transducers 2009:1509–1512

Sarajlic E, Yamahata C, Cordero M, Fujita H (2010) Three-phase electrostatic rotary stepper micromotor with a flexural pivot bearing. IEEE J MEMS 19(2):338–349

Yoshikawa N, Kitagawa K, Takakura S, Takekado S (1996) An Experiment for Head Positioning System Using Submicron Trackwidth GMR head. IEEE Trans On Magn 32(5):3905–3907